Nonclassical photon statistics in cavity QED with an inhomogeneous medium

Hayato Goto and Kouichi Ichimura
Frontier Research Laboratory, Corporate Research and Development Center, Toshiba Corporation, 1, Komukai Toshiba-cho, Saiwai-ku, Kawasaki, 212-8582, Japan

(Received 7 September 2007; published 8 January 2008)

A theoretical method for the calculation of the second-order intensity correlation function for the light transmitted from a weakly driven optical cavity containing an inhomogeneous medium is presented. This method is based on the expectation-value approach [H. Goto and K. Ichimura, Phys. Rev. A **70**, 023815 (2004)]. This method allows one to calculate the second-order intensity correlation function in the case where there are many atoms whose transition frequencies and coupling rates have various values. We discuss the effects of the inhomogeneities of the atomic transition frequency and the coupling rate.

DOI: 10.1103/PhysRevA.77.015804 PACS number(s): 42.50.Ct, 42.50.Ar, 42.50.Dv

It is well known that the light transmitted from an optical cavity coupled to two-level atoms displays nonclassical photon statistics, such as photon antibunching $[g^{(2)}(0) < g^{(2)}(\tau)(\tau \neq 0)]$, sub-Poissonian statistics $[g^{(2)}(0) < 1]$, and the violation of the Schwarz inequality $[|g^{(2)}(0) - 1| < |g^{(2)}(\tau) - 1|(\tau \neq 0)]$ [1,2], where $g^{(2)}(\tau)$ is the second-order intensity correlation function. Since the fully quantum-mechanical treatment of optical bistability [3], the nonclassical photon statistics in cavity quantum electrodynamics (cavity QED) have been well studied theoretically [4–7] and experimentally [8,9]. The photon statistics in cavity QED have also been used for the demonstration of quantum feedback [10].

There are several theoretical approaches to the photon statistics in cavity QED: the Fokker-Planck equation approach [3,4,6], the pure-state approach [5,6], the quantum trajectory approach [2], and the expectation-value approach [7]. In most studies, it has been assumed that the two-level atoms are identical, that is, the atoms have the same values of the transition frequencies and the coupling rates to the cavity. This assumption makes the theoretical treatment much easier. What happens when there are the inhomogeneities of the transition frequency and the coupling rate, that is, the transition frequencies and the coupling rates have various values? To our knowledge, such a situation has not been studied very well so far. Such a situation occurs in the cavity-QED experiment with a rare-earth-metal-ion-doped crystal [11–15]. (Such an experiment is significant for the implementation of quantum computation with a rare-earth-metal-ion-doped crystal [16–18].) In this paper, we present a theoretical method for the calculation of $g^{(2)}(\tau)$ for the light from a cavity coupled to two-level atoms with the above inhomogeneities. This method is based on the expectation-value approach [7]. The expectation-value approach allows one to treat the above complicated problem easily because of its simplicity. We discuss the effects of the inhomogeneities on $g^{(2)}(\tau)$. In this paper, we consider only the weak-field limit. (This is because quantum effects become larger for a weaker field [10], and the expectation-value approach is valid in the weak-field limit [7].) We also neglect the atomic pure dephasing for simplicity [19–22], which was considered in the case of identical atoms in Ref. [7].

The cavity-QED system studied here is described by the following master equation [3,6,7]:

$$\dot{\rho} = \mathcal{L}\rho = -\frac{i}{\hbar}[H_F + H_A + H_I + H_D, \rho] + \mathcal{L}_F\rho + \mathcal{L}_A\rho. \quad (1)$$

Here, ρ is the density operator for the system; the Hamiltonians H_F, H_A, H_I, and H_D, are given by

$$H_F = \hbar\Delta_c a^\dagger a, \quad (2)$$

$$H_A = \hbar\sum_{j=1}^{N} \Delta_j \sigma_z^j, \quad (3)$$

$$H_I = i\hbar\sum_{j=1}^{N} g_j(a^\dagger\sigma_-^j - a\sigma_+^j), \quad (4)$$

$$H_D = i\hbar(\mathcal{E}a^\dagger - \mathcal{E}^* a), \quad (5)$$

where $a^\dagger$ and a are the creation and annihilation operators for the cavity-mode field, $\sigma_\pm^j$ and σ_z^j are the Pauli operators for the jth atom satisfying the commutation relations $[\sigma_+^j, \sigma_-^{j'}] = 2\sigma_z^j\delta_{j,j'}$ and $[\sigma_z^j, \sigma_\pm^{j'}] = \pm\sigma_\pm^j\delta_{j,j'}$, $\mathcal{E}$ is the electric amplitude for the incident field, Δ_c and Δ_j are the detunings of the resonance frequencies of the cavity and the jth atom from the frequency of the incident field, respectively, g_j is the coupling rate between the cavity and the jth atom; the Liouville operators $\mathcal{L}_F$ and $\mathcal{L}_A$ are given by

$$\mathcal{L}_F\rho = \kappa(2a\rho a^\dagger - a^\dagger a\rho - \rho a^\dagger a), \quad (6)$$

$$\mathcal{L}_A\rho = \frac{\gamma}{2}\sum_{j=1}^{N}(2\sigma_-^j\rho\sigma_+^j - \sigma_+^j\sigma_-^j\rho - \rho\sigma_+^j\sigma_-^j), \quad (7)$$

where κ and γ are the decay rates for the cavity field and the atomic excited-state population.

Next, we briefly explain the expectation-value approach to the evaluation of $g^{(2)}(\tau)$ (see Ref. [7] for details). $g^{(2)}(\tau)$ is defined as follows [23]:

$$g^{(2)}(\tau) = \lim_{t\to\infty}\frac{\langle a^\dagger(t)a^\dagger(t+\tau)a(t+\tau)a(t)\rangle}{\langle a^\dagger(t+\tau)a(t+\tau)\rangle\langle a^\dagger(t)a(t)\rangle} \quad (8)$$

 ©2008 The American Physical Society

$$=\frac{\langle a^\dagger(0)a^\dagger(\tau)a(\tau)a(0)\rangle_{\rm SS}}{\langle a^\dagger(0)a(0)\rangle_{\rm SS}^2}, \tag{9}$$

where $\langle O\rangle_{\rm SS}$ is the steady-state expectation value of an operator O, that is, $\langle O\rangle_{\rm SS}={\rm tr}[O\rho_{\rm SS}]$ with the steady-state density operator $\rho_{\rm SS}$. The expectation-value approach is based on the following equation, which is equivalent to Eq. (9) [6,24]:

$$g^{(2)}(\tau)=\frac{\langle a^\dagger(\tau)a(\tau)\rangle_c}{\langle a^\dagger a\rangle_{\rm SS}}, \tag{10}$$

where $\langle O(\tau)\rangle_c$ is the expectation value of O with respect to the following density operator:

$$\rho_c(\tau)=e^{\mathcal{L}\tau}(a\rho_{\rm SS}a^\dagger/\langle a^\dagger a\rangle_{\rm SS}). \tag{11}$$

$\rho_c(\tau)$ describes the state at time $\tau(\tau>0)$ under the condition that the system is in the steady state at $t<0$ and a photon is detected at $t=0$. In general, if an operator-valued vector $\mathbf{A}$ satisfies $\langle\dot{\mathbf{A}}\rangle=M\langle\mathbf{A}\rangle$ (M is a constant coefficient matrix), $\langle\mathbf{A}(\tau)\rangle_c$ can be obtained by

$$\frac{d}{d\tau}\langle\mathbf{A}(\tau)\rangle_c=M\langle\mathbf{A}(\tau)\rangle_c, \tag{12}$$

with the following initial condition:

$$\langle\mathbf{A}(0)\rangle_c=\frac{{\rm tr}[\mathbf{A}a\rho_{\rm SS}a^\dagger]}{\langle a^\dagger a\rangle_{\rm SS}}=\frac{\langle a^\dagger\mathbf{A}a\rangle_{\rm SS}}{\langle a^\dagger a\rangle_{\rm SS}}. \tag{13}$$

Thus, $g^{(2)}(\tau)$ can be obtained by using closed equations for expectation values of operators including $a^\dagger a$ and $a^{\dagger 2}a^2$. This is the expectation-value approach. In order to obtain closed equations, the expectation-value approach assumes a sufficiently weak field.

As mentioned above, the atomic pure dephasing is not considered in this paper. As a result, the following relations hold: $\langle A^\dagger B\rangle_{\rm SS}=\langle A^\dagger\rangle_{\rm SS}\langle B\rangle_{\rm SS}$ and $\langle A^\dagger(\tau)B(\tau)\rangle_c=\langle A^\dagger(\tau)\rangle_c\langle B(\tau)\rangle_c$, where both A and B are operators composed of a and σ_-^j [25]. Therefore, $g^{(2)}(\tau)$ can be obtained from the following simpler equation than Eq. (10):

$$g^{(2)}(\tau)=\frac{\langle a^\dagger(\tau)\rangle_c\langle a(\tau)\rangle_c}{\langle a^\dagger\rangle_{\rm SS}\langle a\rangle_{\rm SS}}=\left|\frac{\langle a(\tau)\rangle_c}{\langle a\rangle_{\rm SS}}\right|^2. \tag{14}$$

Thus, $g^{(2)}(\tau)$ can be obtained by using closed equations for expectation values of operators including a and a^2, instead of $a^\dagger a$ and $a^{\dagger 2}a^2$.

Such closed equations are as follows [26]:

$$\frac{d}{dt}\langle a\rangle=-\tilde{\kappa}\langle a\rangle+\sum_{j=1}^{N}g_j\langle\sigma_-^j\rangle+\mathcal{E}, \tag{15}$$

$$\frac{d}{dt}\langle\sigma_-^j\rangle=-\frac{\tilde{\gamma}_j}{2}\langle\sigma_-^j\rangle-g_j\langle a\rangle, \tag{16}$$

$$\frac{d}{dt}\langle a^2\rangle=-2\tilde{\kappa}\langle a^2\rangle+2\sum_{j=1}^{N}g_j\langle a\sigma_-^j\rangle+2\mathcal{E}\langle a\rangle, \tag{17}$$

$$\frac{d}{dt}\langle a\sigma_-^j\rangle=-\left(\tilde{\kappa}+\frac{\tilde{\gamma}_j}{2}\right)\langle a\sigma_-^j\rangle-g_j\langle a^2\rangle+\sum_{j'=1}^{N}g_{j'}\langle\sigma_-^j\sigma_-^{j'}\rangle+\mathcal{E}\langle\sigma_-^j\rangle, \tag{18}$$

$$\frac{d}{dt}\langle\sigma_-^j\sigma_-^{j'}\rangle=-\frac{\tilde{\gamma}_j+\tilde{\gamma}_{j'}}{2}\langle\sigma_-^j\sigma_-^{j'}\rangle-(g_{j'}\langle a\sigma_-^j\rangle+g_j\langle a\sigma_-^{j'}\rangle)+2g_j\langle a\sigma_-^j\rangle\delta_{j,j'}, \tag{19}$$

where $\tilde{\kappa}\equiv\kappa+i\Delta_c$ and $\tilde{\gamma}_j\equiv\gamma+2i\Delta_j$. The steady-state solution for Eqs. (15)–(19) is easily obtained by using the following equation for $\langle a\sigma_-^j\rangle_{\rm SS}$, which is obtained by substituting Eqs. (17) and (19) into Eq. (18):

$$\left(\tilde{\kappa}+\frac{\tilde{\gamma}_j}{2}+\sum_{j'=1}^{N}\frac{2g_jg_{j'}}{\tilde{\gamma}_j+\tilde{\gamma}_{j'}}-\frac{2g_j^2}{\tilde{\gamma}_j}\right)\langle a\sigma_-^j\rangle_{\rm SS}+\sum_{j'=1}^{N}\left(\frac{2g_jg_{j'}}{\tilde{\gamma}_j+\tilde{\gamma}_{j'}}+\frac{g_jg_{j'}}{\tilde{\kappa}}\right)\langle a\sigma_-^{j'}\rangle_{\rm SS}=-\mathcal{E}\langle a\rangle_{\rm SS}\left(\frac{g_j}{\tilde{\kappa}}+\frac{2g_j}{\tilde{\gamma}_j}\right). \tag{20}$$

$\langle a(\tau)\rangle_c$ can be obtained by numerically solving the differential equations (15) and (16) with the following initial condition:

$$\langle a(0)\rangle=\frac{\langle a^2\rangle_{\rm SS}}{\langle a\rangle_{\rm SS}}, \tag{21}$$

$$\langle\sigma_-^j(0)\rangle=\frac{\langle a\sigma_-^j\rangle_{\rm SS}}{\langle a\rangle_{\rm SS}}. \tag{22}$$

Thus, $\langle a\rangle_{\rm SS}$ and $\langle a(\tau)\rangle_c$ can be calculated, and $g^{(2)}(\tau)$ is obtained from Eq. (14) even in the case where there are many atoms whose transition frequency and coupling rate have various values.

What is interesting may be the effects of the above inhomogeneities on $g^{(2)}(\tau)$. To discuss the effect of the inhomogeneity of the atomic detuning, we first calculated $g^{(2)}(\tau)$ in the case where the atomic detuning was regularly distributed as follows [27]:

$$\Delta_j=-50\gamma\left(1-2\frac{j-1}{N-1}\right)(j=1,2,\ldots,N). \tag{23}$$

The solid, dashed, and dotted curves in Fig. 1(a) show $g^{(2)}(\tau)$ in the cases where the atomic number N was set to 21, 51, and 101, respectively. The distributions of (Δ_j,g_j) in these cases are shown in Figs. 1(b)–1(d), respectively. The other parameters were set as $\kappa/\gamma=50$ and $\Delta_c=0$.

For comparison, we also show $g^{(2)}(\tau)$ in the single-atom case in Fig. 2. The solid, dashed, and dotted curves in Fig. 2(a) show $g^{(2)}(\tau)$ in the cases where the atomic detuning was set as $\Delta_1=0$, $\gamma/4$, and $\gamma/2$, respectively. The solid, dashed, and dotted curves in Fig. 2(b) show $g^{(2)}(\tau)$ in the cases where $\Delta_1=\gamma$, 2γ, and 5γ, respectively. The other parameters were set as $g_1/\gamma=5$, $\kappa/\gamma=50$, and $\Delta_c=0$. When $\Delta_1>5\gamma$, $g^{(2)}(\tau)\simeq 1$ for all τ.

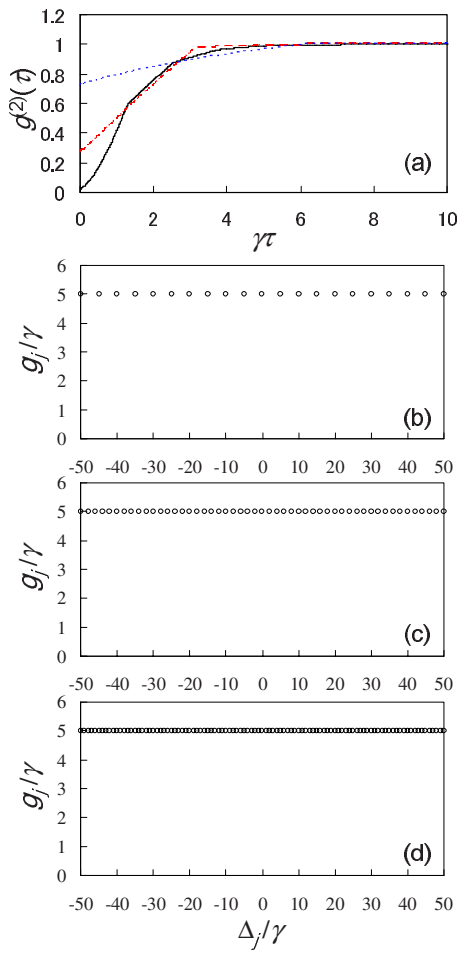

FIG. 1. (Color online) $g^{(2)}(\tau)$ vs $\gamma\tau$ in the case where Δ_j are regularly distributed. The solid, dashed, and dotted curves in (a) correspond to the cases where (Δ_j, g_j) are set as shown in (b), (c), and (d), respectively. The atomic number is (b) $N=21$, (c) $N=51$, and (d) $N=101$. The other parameters were set as $\kappa/\gamma=50$ and $\Delta_c=0$.

Since there is a single atom whose detuning is equal to zero in all the cases of Fig. 1, the difference between the curves in Fig. 1(a) and the solid curve in Fig. 2(a) is due to the atoms with nonzero detuning. First of all, the solid curve in Fig. 1(a) is very similar to the solid curve in Fig. 2(a). This means that the effect of the atoms with nonzero detuning is quite small in the case of Fig. 1(b) ($N=21$). On the other hand, Fig. 1(a) shows that higher atomic density leads to smaller nonclassicality [28,29]. This may come from the larger contribution of the atoms with nonzero detuning. (The atoms with nonzero detuning induce photon bunching as indicated in Fig. 2.) If the atomic density is sufficiently high, the nonclassicality may vanish, which was also indicated by the other calculated result [30]. (This means that the effect of the atoms with detuning near to zero is cancelled by that of the atoms with relatively large detuning.) This may also be the case for uniform distribution of the detuning other than that defined by Eq. (23). (This is because individual values of the detuning may be unimportant when the density is sufficiently high.)

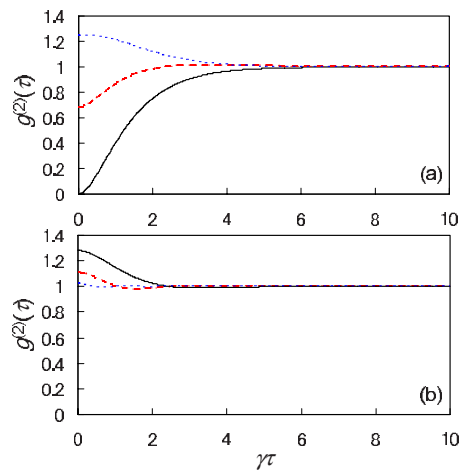

FIG. 2. (Color online) $g^{(2)}(\tau)$ vs $\gamma\tau$ in the single-atom case. Solid curve in (a) $\Delta_1=0$. Dashed curve in (a) $\Delta_1=\gamma/4$. Dotted curve in (a) $\Delta_1=\gamma/2$. Solid curve in (b) $\Delta_1=\gamma$. Dashed curve in (b) $\Delta_1=2\gamma$. Dotted curve in (b) $\Delta_1=5\gamma$. The other parameters were set as $g_1/\gamma=5$, $\kappa/\gamma=50$, and $\Delta_c=0$.

Finally, we examine the cases where the atomic detuning or the coupling rate is randomly distributed. The atomic number was set as $N=101$. The solid curve in Fig. 3(a) shows $g^{(2)}(\tau)$ in the case where g_j are randomly distributed in the range from 0 to 5γ except an atom with zero detuning. The coupling rate for the atom with zero detuning was set to

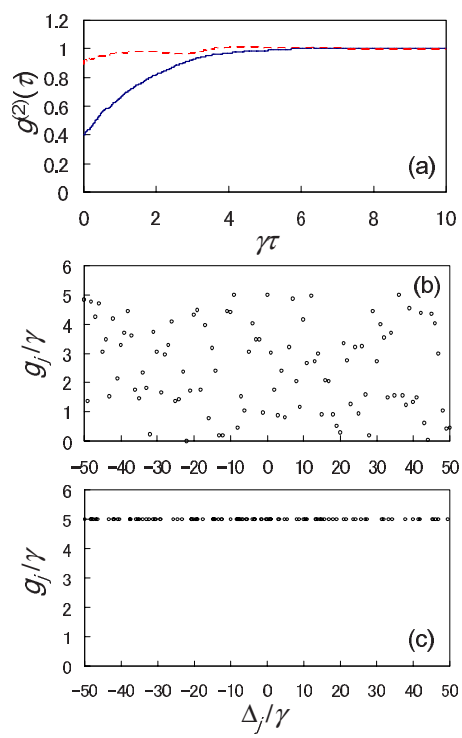

FIG. 3. (Color online) $g^{(2)}(\tau)$ vs $\gamma\tau$ in the case where g_j or Δ_j are randomly distributed. The atomic number was set as $N=101$. The solid and dashed curves in (a) correspond to the cases where (Δ_j, g_j) are set as shown in (b) and (c), respectively. The other parameters were set as $\kappa/\gamma=50$ and $\Delta_c=0$.

5γ. Δ_j were defined as Eq. (23). This distribution of (Δ_j, g_j) is shown in Fig. 3(b). The other parameters were set as $\kappa/\gamma=50$ and $\Delta_c=0$. The nonclassicality in the case of Fig. 3(b) is larger than that in the case of Fig. 1(d). This result may come from the smaller coupling rates for the atoms with nonzero detuning. On the other hand, the dashed curve in Fig. 3(a) shows $g^{(2)}(\tau)$ in the case where Δ_j are randomly distributed in the range from -50γ to 50γ except an atom with zero detuning ($\Delta_1=0$). g_j were set to 5γ. This distribution of (Δ_j, g_j) is shown in Fig. 3(c). The other parameters were set as $\kappa/\gamma=50$ and $\Delta_c=0$. The nonclassicality in the case of Fig. 3(c) is smaller than that in the case of Fig. 1(d). This result may come from the larger number of the atoms with small but nonzero detuning [31].

In conclusion, we have presented a theoretical method for the calculation of the second-order intensity correlation function $g^{(2)}(\tau)$ for the light from a cavity coupled to two-level atoms whose transition frequencies and coupling rates have various values. This is based on the expectation-value approach [7]. This method will be useful for the analysis of the cavity-QED experiment with a rare-earth-metal-ion-doped crystal. We have calculated $g^{(2)}(\tau)$ in several cases to examine the effects of the inhomogeneities on $g^{(2)}(\tau)$. It has been found that the larger number of atoms with nonzero detuning leads to smaller nonclassicality, and the nonclassicality may vanish for sufficiently high atomic density in the case of uniform distribution of the atomic detuning. All the results presented here have been explained well with $g^{(2)}(\tau)$ in the single-atom case. There are two interesting open questions: whether or not there is an case in which $g^{(2)}(\tau)$ in the case of the inhomogeneities cannot be explained very well with $g^{(2)}(\tau)$ in the single-atom case; whether or not there is a case in which the nonclassicality remains even for high atomic density. The present method can be used to investigate these problems.

[1] P. R. Rice and H. J. Carmichael, IEEE J. Quantum Electron. **24**, 1351 (1988).
[2] J. P. Clemens and P. R. Rice, Phys. Rev. A **61**, 063810 (2000).
[3] P. D. Drummond and D. F. Walls, Phys. Rev. A **23**, 2563 (1981).
[4] H. J. Carmichael, Phys. Rev. A **33**, 3262 (1986).
[5] H. J. Carmichael, R. J. Brecha, and P. R. Rice, Opt. Commun. **82**, 73 (1991).
[6] R. J. Brecha, P. R. Rice, and M. Xiao, Phys. Rev. A **59**, 2392 (1999).
[7] H. Goto and K. Ichimura, Phys. Rev. A **70**, 023815 (2004); **74**, 069901(E) (2006).
[8] G. Rempe, R. J. Thompson, R. J. Brecha, W. D. Lee, and H. J. Kimble, Phys. Rev. Lett. **67**, 1727 (1991).
[9] G. T. Foster, S. L. Mielke, and L. A. Orozco, Phys. Rev. A **61**, 053821 (2000).
[10] J. E. Reiner, W. P. Smith, L. A. Orozco, H. M. Wiseman, and J. Gambetta, Phys. Rev. A **70**, 023819 (2004).
[11] C. Greiner, B. Boggs, and T. W. Mossberg, Phys. Rev. Lett. **85**, 3793 (2000).
[12] C. Greiner, T. Wang, T. Loftus, and T. W. Mossberg, Phys. Rev. Lett. **87**, 253602 (2001).
[13] C. Greiner, B. Boggs, and T. W. Mossberg, Phys. Rev. A **67**, 063811 (2003).
[14] K. Ichimura and H. Goto, Phys. Rev. A **74**, 033818 (2006).
[15] The linewidth of rare-earth-metal ions in a crystal is inhomogeneously broadened. This induces the inhomogeneity of the transition frequency. On the other hand, such ions are randomly positioned in a crystal. This induces the inhomogeneity of the coupling rate because the coupling rate for an ion depends on the position of the ion.
[16] K. Ichimura, Opt. Commun. **196**, 119 (2001).
[17] M. S. Shahriar, J. A. Bowers, B. Demsky, P. S. Bhatia, S. Lloyd, P. R. Hemmer, and A. E. Craig, Opt. Commun. **195**, 411 (2001).
[18] H. Goto and K. Ichimura, Phys. Rev. A, **70**, 012305 (2004).
[19] The pure dephasing in rare-earth-metal-ion-doped crystals is negligible in the cases of $Eu^{3+}:Y_2SiO_5$ [20,21] and the application of an external magnetic field [22].
[20] R. Yano, M. Mitsunaga, and N. Uesugi, Opt. Lett. **16**, 1884 (1991).
[21] R. W. Equall, Y. Sun, R. L. Cone, and R. M. Macfarlane, Phys. Rev. Lett. **72**, 2179 (1994).
[22] Y. Sun, C. W. Thiel, R. L. Cone, R. W. Equall, and R. L. Hutcheson, J. Lumin. **98**, 281 (2002).
[23] H. J. Carmichael, *Statistical Methods in Quantum Optics 1* (Springer-Verlag, Berlin, 1999).
[24] This is also the basis for the standard method of the measurement of $g^{(2)}(\tau)$ with the delay-time measurement of two photons.
[25] These are found from the fact that the differential equations for $\langle A^\dagger B\rangle$ is the same as $\langle A^\dagger\rangle\langle B\rangle$.
[26] These are derived from the master equation (1) and in the weak-field limit.
[27] The range of Δ_j was set as this because we have confirmed by numerical calculation that in the present case atoms with a detuning larger than 50γ ($|\Delta_j|>50\gamma$) do not contribute to $g^{(2)}(\tau)$.
[28] In this paper, we say that nonclassicality is larger when $g^{(2)}(0)$ is smaller, because photon antibunching and sub-Poissonian photon statistics are defined as $g^{(2)}(0)<g^{(2)}(\tau)(\tau\neq 0)$ and $g^{(2)}(0)<1$, respectively.
[29] It should be noted that in general the limit of large atomic number does not necessarily lead to classical statistics. This fact is obvious from the analytic result in the case of identical atoms [5,7].
[30] We confirmed that $g^{(2)}(\tau)$ was approximately equal to 1 for all τ when the atomic density was ten times higher than that in the case of Fig. 1(d), where the atomic detuning was defined as $\Delta_j=-5\gamma[1-2(j-1)/100]$ $(j=1,2,\ldots,101)$.
[31] The numbers of the atoms with detuning smaller than 5γ but not equal to zero ($0<|\Delta_j|<5\gamma$) are 8 and 13 in the cases of Figs. 1(d) and 3(c), respectively.